

In Vitro Characterization and Pharmacokinetics of Dapagliflozin (BMS-512148), a Potent Sodium-Glucose Cotransporter Type II (SGLT2) Inhibitor, in Animals and Humans

M. OBERMEIER, M. YAO, A. KHANNA, B. KOPLOWITZ, M. ZHU, W. LI, B. KOMOROSKI, S. KASICHAYANULA, L. DISCENZA, W. WASHBURN, W. MENG, B. A. ELLSWORTH, J. M. WHALEY, W. G. HUMPHREYS

Department of Pharmaceutical Candidate Optimization- Metabolism and Pharmacokinetics (M.O.), Department of Pharmaceutical Candidate Optimization-Development Biotransformation (M.Y., M.Z., W.L., W.G.H.), SV Life Sciences LLC, Foster City, CA (A.K), Duck Flats Pharma, Elbridge, NY (B.Kop.), Department of Global Marketing (B.Kom.), Department of Discovery Medicine and Clinical Pharmacology (S.K.), Department of Pharmaceutical Candidate Optimization-Bioanalytical Research (L.D.), Department of Metabolic Diseases Biology (J.W.), and Department of Metabolic Diseases Chemistry (W.W., W.M., B.A.E.), Bristol-Myers Squibb Pharmaceutical Research Institute, Princeton, NJ, USA

Running title

In Vitro Metabolism and Pharmacokinetics of Dapagliflozin

Mary T. Obermeier, Bristol-Myers Squibb Co., P.O. Box 4000, Princeton, NJ 08543.
Phone 609-252-3817, Fax 609-252-6802
Email: mary.obermeier@bms.com

Number of text pages: 34 (starting with Introduction)

Number of Tables: 1

Number of Figures: 7

Number of references: 30

Number of words in Abstract: 218

Number of words in Introduction: 818

Number of words in Discussion: 1010

List of Abbreviations:

ACN: acetonitrile

ADME: absorption, distribution, metabolism, and excretion

AUC: area under the concentration/time curve

AUMC: area under the moment curve

BQL: below quantifiable limit

BW: body weight

CL: total body clearance

CL_R: renal clearance

CPM: counts per minute

CYP: Cytochrome P450

Da: daltons

DMSO: dimethyl sulfoxide

EDTA: ethylene diamine tetraacetic acid

F: oral bioavailability

fu: fraction unbound

GFR: glomerular filtration rate

HbA1c: glycosylated hemoglobin
HLM: human liver microsomes
HPLC: high performance liquid chromatography
IA: intraarterial
IV: intravenous
KCl: potassium chloride
LC/MS/MS: liquid chromatography: mass spectroscopy
LSC: liquid scintillation counting
MAD: multiple ascending dose
MRM: multiple reaction monitoring
mRNA: messenger ribonucleic acid
MRT: mean residence time
NADPH: nicotinamide adenine dinucleotide phosphate, reduced form
NH₃: ammonia
ODS: octyl dodecyl sulfate, C18
P-gp: P-glycoprotein
PO: *per os.*, oral
RT: room temperature
SAD: single ascending dose
SGLT: sodium-glucose cotransporter
SPE: solid phase extraction
SRM: selective reaction monitoring
T_{max}: time that peak concentrations are reached
TRA: total radioactivity
UDPGA: uridine diphosphoglucuronic acid
UV: ultraviolet
V_{ss}: volume of distribution at steady state

ABSTRACT:

Dapagliflozin (2*S*,3*R*,4*R*,5*S*,6*R*)-2-(3-(4-Ethoxybenzyl)-4-chlorophenyl)-6-hydroxymethyl-tetrahydro-2*H*-pyran-3,4,5-triol; BMS-512148) is a potent sodium-glucose cotransporter type II inhibitor in animals and humans and is currently under development for the treatment of type 2 diabetes. The preclinical characterization of dapagliflozin, to allow compound selection and prediction of pharmacological and dispositional behavior in the clinic, involved Caco-2 cell permeability studies, CYP inhibition and induction studies, CYP reaction phenotyping, metabolite identification in hepatocytes and pharmacokinetics in rats, dogs, and monkeys. Dapagliflozin was found to have good permeability across Caco-2 cell membranes. It was found to be a substrate for P-glycoprotein (P-gp) but not a significant P-gp inhibitor. Dapagliflozin was not found to be an inhibitor or an inducer of human CYP enzymes. The in vitro metabolic profiles of dapagliflozin after incubation with hepatocytes from mice, rats, dogs, monkeys, and humans were qualitatively similar. Rat hepatocyte incubations showed the highest turnover and dapagliflozin was most stable in human hepatocytes. Prominent in vitro metabolic pathways observed were glucuronidation, hydroxylation, and O-deethylation. Pharmacokinetic parameters for dapagliflozin in preclinical species revealed a compound with adequate oral exposure, clearance, and elimination half-life, consistent with the potential for single daily dosing in humans. Indeed, the pharmacokinetics in humans after a single dose of 50 mg of [¹⁴C]dapagliflozin showed good exposure, low clearance, adequate half-life, and no metabolites with significant pharmacological activity or toxicological concern.

Introduction

Type 2 diabetes mellitus is a chronic disease prevalent around the world, characterized by hyperglycemia due to excessive hepatic glucose production, a deficiency in insulin secretion and/or peripheral insulin resistance. As the disease advances, complications result from the hyperglycemia, such as retinopathy, neuropathy, nephropathy and other macrovascular diseases (Porte, 2001; Edelman, 1998). While present antidiabetic agents can achieve the needed reduction in plasma glucose, no single current medication is optimal to achieve sustained glycemic control without side effects, such as hypoglycemia. And the often necessary combination therapy can generate additional side effects. For example, treatment with thiazolidinediones (glitazones) in combination with insulin are related to an increased risk of congestive heart failure due to edema events (Nesto et al., 2004). There are very few therapies, with the exception of the novel dipeptidyl peptidase 4 (DPP-4) inhibition, that do not cause an increase in body weight or risk of hypoglycemia (Barnett, 2006). In addition, agents that increase the production of insulin stress the pancreatic beta cells, which results in eventual hypertrophy and loss of differentiation of those cells, contributing to the progression of the disease (List, et.al., 2008).

Thus, the development of alternative agents acting by novel mechanisms has become necessary in order to control glucose levels in patients with progressing hyperglycemia (Rotella, 2004; Skyler, 2004; Mohler et al., 2008;). Some emerging small molecules primarily lower blood glucose levels by modulating targets that affect glucose metabolism (glucokinase, glycogen phosphorylase) or by regulating glucose homeostasis (AMP activated protein kinase). One such novel mechanism by which blood glucose levels can be

lowered is by removing glucose from the bloodstream via inhibition of the sodium glucose co-transporter SGLT.

Under normal conditions, plasma glucose is filtered in the kidney glomerulus and in healthy individuals is almost totally (99%) reabsorbed (Deetjen et al., 1992). This reabsorption process is mediated by two sodium-dependent glucose cotransporters- SGLT1 and SGLT2. SGLT1 is a low capacity, high-affinity transporter expressed in the gut, heart, and kidney (Wright et al., 1993), and SGLT2 is a high-capacity, low-affinity transporter expressed mainly in the S1 segment of the proximal tubule of the nephron (Kanai, et al., 1994). The SGLT2 in the proximal tubule is estimated to facilitate about 90% of renal glucose reabsorption, and the remaining 10% is likely mediated by SGLT1 that resides in the distal S3 segment of the proximal tubule (Wallner, et al., 2001).

Nonselective SGLT inhibitors have been described, such as the natural product phlorizin (Ehrenkranz et al., 2005), which is an *O*-glucoside dihydrochalcone found in the root and bark of certain fruit trees. Phlorizin was not suitable for development as a drug candidate due to low bioavailability and rapid clearance as a consequence of hydrolysis by *O*-glucosidases present in the gut, liver and kidney. In addition, the finding that a defective SGLT1 transporter in the gut is responsible for glucose and galactose malabsorption disorders in patients (Turk et al., 1991) suggests that pursuit of SGLT2 inhibitors exhibiting comparable (less than tenfold) SGLT1 selectivity to phlorizin would increase the risk of unacceptable diarrhea.

Selective inhibition of SGLT2 has been proposed to aid in the normalization of plasma glucose levels in diabetics by preventing the renal glucose reabsorption process and promoting glucose excretion in urine (Oku et al., 1999). Dapagliflozin is a potent, selective

SGLT2 inhibitor in vitro, and also demonstrates increased glucose excretion and highly efficacious plasma glucose lowering in preclinical species (Han et al., 2008; Meng et al., 2008). Dapagliflozin is not only selective for SGLT2 (1200-fold over SGLT1) but is also more metabolically stable than previously described SGLT inhibitors since it is a *C*-glucoside rather than an *O*-glucoside (Ellsworth et al., 2008; Meng et al., 2008). Proof of concept and phase 2b studies in patients with type 2 diabetes have been conducted with various doses of dapagliflozin and published previously (List et al., 2008; Komoroski et al., 2009 (a); Komoroski et al., 2009 (b)). Dapagliflozin exhibits an insulin-independent mechanism of action, providing both short term and longer term (HbA1c levels) efficacy (List et al., 2008). In studies with the SGLT inhibitor phlorizin, this insulin-independent mechanism was shown to alleviate the loss of beta cell function, normalizing the blood glucose levels without increasing plasma insulin or changing levels of nonesterified fatty acids in plasma (Jonas et al., 1999).

Once *C*-glycoside SGLT2 inhibitors were identified as being pharmacologically attractive compounds, with very good selectivity for the target, and potency in both in vitro and in vivo assessments, studies were conducted to characterize the in vitro absorption, metabolism, drug-drug interaction potential, and pharmacokinetics in mice, rats, dogs, and monkeys, to aid in compound selection. Based on the data from these evaluations, dapagliflozin was selected for progression into clinical trials and the ADME-related data is presented in this manuscript. As dapagliflozin progressed as the development candidate, a mass balance study with radiolabeled dapagliflozin was conducted in healthy volunteers, and some brief results from that study are also reported here.

Materials and Methods

Chemicals and Equipment. Dapagliflozin (2*S*,3*R*,4*R*,5*S*,6*R*)-2-(3-(4-Ethoxybenzyl)-4-chlorophenyl)-6-hydroxymethyl-tetrahydro-2*H*-pyran-3,4,5-triol; BMS-512148), and a chemical standard corresponding to the *O*-deethylated metabolite (M8), were synthesized at Bristol-Myers Squibb Co. and were at least 99% pure based on HPLC purity analysis. A standard of hydroxylated metabolite (M12) was purified from a large scale incubation of dapagliflozin with rat liver microsomes. The structures of these reference standards are shown in Figure 3. Structural characterization data for dapagliflozin and synthesized or purified metabolites can be found in Supplemental Data. [¹⁴C]Dapagliflozin (specific activity of 2.07 μCi/mg and a radiochemical purity of 99.5%) was synthesized in the Bristol-Myers Squibb Radiochemistry Department, New Brunswick, NJ. The position of the ¹⁴C-label is shown in Figure 3. All other chemicals were reagent grade or better, and were obtained from Sigma-Aldrich Chemical Co. (St. Louis, MO) unless otherwise specified. For the Caco-2 permeability and protein binding studies, 24-well plates were obtained from Corning Inc. (Corning, NY). Caco-2 cells were obtained from American Type Culture Collection (Rockville, MD). Dulbecco's modified Eagle's medium, nonessential amino acids, L-glutamine, penicillin-G, and streptomycin were purchased from JHR Biosciences (Lenexa, KS). Fetal bovine serum was obtained from Hyclone Lab. Inc. (Logan, Utah). Rat tail collagen-type I was purchased from Collaborative Research Inc. (Bedford, MA). HTS-Transwell® inserts (surface area: 1 cm²) with a polycarbonate membrane (0.4 μm pore size) were purchased from Costar (Cambridge, MA). Verapamil was obtained from Sigma-Aldrich Chemical Co. (St. Louis, MO).

Control blood from rat, dog, monkey, and human; control plasma from rat, dog, and human; and control monkey serum were obtained from Bioreclamation (Hicksville, NY). For the CYP inhibition studies, midazolam, 1-hydroxymidazolam, (*S*)-mephenytoin, (*S*)-4'-hydroxymephenytoin, hydroxybupropion, 6 α -hydroxypaclitaxel, and pooled human liver microsomes (HLM) were obtained from BD Biosciences (Woburn, MA, USA). EcoliteTM liquid scintillation cocktail was purchased from MP Biomedicals, Inc., Irvine, CA. Cryopreserved hepatocytes from male Sprague-Dawley rat, male beagle dog, male cynomolgus monkey, and human (3 donors) were obtained from In Vitro Technologies (Baltimore, MD). Balb/C mouse hepatocytes were prepared in BMS laboratories using standard techniques (Seglen, 1976) and used on the day of isolation. For analysis of radioactivity in samples from the hepatocyte incubations used for metabolite identification, a TopCount NXTTM microplate scintillation and luminescence counter (Perkin Elmer Inc., Downers Grove, IL) was used.

For the cytochrome P450 (CYP) induction studies, phosphate buffered saline, tissue culture media (DMEM and Chee's) and additives were purchased from Invitrogen (Gibco, Grand Island, NY). Extracellular matrix proteins (collagen Type 1 and matrigel) were purchased from BD Biosciences (Bedford, MA) and culture dishes (60-mm Permanox®) were obtained from NUNC (Naperville, IL). Lactate dehydrogenase (LDH) assay kit was purchased from Promega (Madison, WI). For the CYP induction assay, the substrates, metabolites and internal standards included: phenacetin, acetaminophen (APAP), *N*-(4-hydroxyphenyl-2,3,5,6-*d*4) acetamide, bupropion, hydroxybupropion (OHBP; obtained from BD Biosciences, Woburn, MA), testosterone and 6 β -hydroxytestosterone (6 β T) were obtained from Sigma/Aldrich Chemical Co.

Animals. All procedures involving animals and their care were conducted in conformity with the guidelines that are in compliance with the Bristol-Myers Squibb Institutional Animal Care and Use Committee. Adult male Sprague-Dawley rats (200-283 g) were obtained from Harlan Sprague-Dawley (Indianapolis, IN, USA). Rats were surgically prepared with indwelling jugular vein cannulae (oral animals), or indwelling jugular vein cannulae and carotid artery cannulae (intra-arterial animals), one day before drug administration. Adult male beagle dogs (11.6-14.8 kg) were from an in-house colony. Those that received the intravenous doses had chronically implanted femoral vein access ports. Adult male cynomolgus monkeys (6.2-7.1 kg) were from an in-house colony. All the monkeys used had chronically implanted femoral vein access ports. All animals were fasted overnight prior to dosing and were fed 4 h after dosing. All animals had free access to water and were conscious throughout the study.

Drug. For all pharmacokinetic studies in animals, dapagliflozin was formulated in polyethylene glycol (PEG 400): water: ethanol (45:45:10, v:v:v) at a concentration of 1 mg/mL.

Drug Treatment. Two groups of three rats each were given a single oral or intraarterial dose of dapagliflozin (1 mg/kg). A single dose of dapagliflozin (6.6 mg/kg) was administered orally and intravenously to three beagle dogs in a crossover fashion. In an analogous crossover study, dapagliflozin (6 mg/kg) was administered orally and intravenously to three cynomolgus monkeys.

Sampling. For rats, blood samples were collected from the jugular vein cannulae, at 10 and 30 min, and 1, 2, 4, 6, 8, and 12 h after both the intraarterial and oral administration.

For dogs and monkeys, blood samples were collected from the jugular vein, at 10, 15, 30, and 45 min, and 1, 2, 4, 6, 8, 12, 24, 32, and 48 h after intravenous administration; and at 15, 30, and 45 min, and 1, 2, 4, 6, 8, 12, 24, 32, and 48 h after oral administration. All blood samples were collected into syringes containing potassium ethylenediamine tetraacetic acid (K₃EDTA) salt. The plasma fraction was immediately separated by centrifugation (14,000xg, 10 min, 4°C), frozen on dry ice, and stored at -20°C until the samples were analyzed. For dogs and monkeys, urine was also collected over the duration of the study. Plasma and urine samples were treated with two volumes of ACN containing internal standard. After centrifugation to remove precipitated proteins, an aliquot of supernatant was analyzed by LC/MS/MS.

Clinical Study. The protocol, amendments, and informed consent for this study were approved by the Institutional Review Board (IRB)/ Independent Ethics Committee (IEC), and conducted in accordance with good clinical practices (GCP). Six healthy adult males were enrolled in an open-label, non-randomized, single-dose study. Subjects were given a single oral dose of 50 mg of [¹⁴C]dapagliflozin solution, containing approximately 125 µCi of total radioactivity (TRA). The dose volume was 10 mL (5 mg/mL in PEG400:water (30:70, v:v) solution, and was followed by the administration of 240 mL of water. Blood samples were collected from an indwelling catheter or by direct venipuncture into tubes containing K₂EDTA, at 0.25, 0.5, 0.75, 1, 1.5, 2, 2.5, 3, 4, 6, 8, 12, 24, 36, 48, 72, 96, 120, 144, 168, 192, 216, 240, 264, 288, and 312 h. Blood samples was centrifuged for 15 min at 1000xg to obtain plasma, and stored at -20°C until analysis for TRA and dapagliflozin concentrations by a validated LC/MS/MS method. Additional blood samples were

obtained at 1, 4, 12, 48, and 144 h after the dose, for biotransformation analysis. Urine and feces were also collected. Urine was collected in chilled urine collection jugs and stored refrigerated during the collection period (0-12 and 12-24 h on day 1, then every 24 h on subsequent days). Aliquots taken for TRA and drug analysis and remaining bulk urine were stored at -70°C until analysis.

In Vitro Studies. *Caco-2 permeability studies and P-gp interaction studies.* Caco-2 cells were seeded onto 12 well polycarbonate filter membrane at a density of 60,000 cells/cm². The permeability studies were conducted as described previously (Kamath et al., 2008), but with the addition of a potent inhibitor of P-gp (GF-120918, 4 µM), to both the apical and the basolateral compartments in the bi-directional permeability studies. The ability of dapagliflozin to inhibit P-gp was evaluated by assessing the inhibition of the transport of digoxin, a P-gp substrate, through Caco-2 cell monolayers, and was conducted as described previously (Kamath et al., 2008).

Plasma protein binding. The protein binding of dapagliflozin in rat, dog, and human plasma was determined in a 96-well equilibrium dialysis apparatus using dialysis membranes with a 12,000- to 14,000-dalton molecular weight cutoff (HTDialysis, LLC, Gales Ferry, CT). The dialysis buffer was 0.133 M sodium phosphate buffer (pH 7.4). Plasma (previously frozen) was spiked with dapagliflozin (1 mM in ACN) to achieve final concentrations of 10 µM. The dialysis was conducted in triplicate for 4 h at 37°C. Aliquots of plasma dialysates were analyzed using an LC/MS/MS method. The unbound fraction (f_u) was calculated as the concentration of dapagliflozin in the plasma dialysate

divided by the concentration in the spiked plasma. Values are reported as means \pm S.D. for three determinations.

Serum protein binding. The in vitro protein binding of dapagliflozin in monkey serum was determined by ultrafiltration using Centrifree[®] UP devices with a molecular mass cutoff of $>30,000$ Da (Millipore, Billerica, MA). Dapagliflozin (1 mM in ACN) was added to serum in triplicate to yield final concentrations of 10 μ M. The serum binding study was conducted at room temperature. After the spiked serum samples were added to the filtration devices, they were centrifuged at a 33° fixed angle for 15 min at 10,000xg. Aliquots of serum ultrafiltrate were analyzed using an LC/MS/MS method. The unbound fraction (f_u) was calculated as the concentration of dapagliflozin in the serum ultrafiltrate divided by the concentration in the spiked serum. Values are reported as means \pm S.D. for three determinations.

Blood cell partitioning. Dapagliflozin (1 mM in ACN) was added to samples of rat, dog, and monkey blood, in triplicate, to yield final concentrations of 10 μ M. Samples were incubated, in triplicate, at 37°C in a shaking water bath for 2 h. For testing in human blood, 0.5 mM of dapagliflozin in ACN:water (1:1, v/v) was added to samples of human blood, in triplicate, to yield a final concentration of 5 μ M, and these samples were incubated at 37°C in an incubator containing 95% O₂:5% CO₂ for 2 h. Aliquots of blood were removed at 2 hours and split into two portions. One portion was treated with an equal volume of water and centrifuged to obtain supernatant. The remaining blood was centrifuged to obtain plasma. Samples were analyzed using LC/MS/MS. A blood to

plasma partitioning ratio (C_B/C_P) for dapagliflozin was calculated from the concentrations in blood (C_B) and plasma (C_P).

CYP inhibition studies in pooled human liver microsomes. A stock solution (30 mM) was prepared by dissolving dapagliflozin in DMSO and was stored at 2-8°C prior to preparation of solutions of dapagliflozin at concentrations of 0, 0.0045, 0.018, 0.09, 0.36, 1.8, 9 and 45 μ M. To determine the IC_{50} values, HLM (Lot BMS022, pooled from 19 individuals, and Lot No. 27, pooled from 38 individuals; 0.05~0.25 mg/mL microsomal protein) were incubated in triplicate as described previously (Yao et al., 2007).

CYP induction studies in hepatocytes and sample analysis. Primary cultures of human hepatocytes were prepared at CellzDirect from human liver tissue from three donors (Hu472, Hu476, and Hu477). The CYP induction studies were conducted by CellzDirect (Pittsboro, NC), and a brief description of the study is shown below. A fresh stock solution of dapagliflozin was prepared in DMSO on the first day of dosing. Stock solutions were diluted daily in modified Chee's medium to achieve the final dosing concentrations of 0.2, 2 and 20 μ M for dapagliflozin and a final DMSO concentration of 0.1%. Primary human hepatocytes were prepared from human liver tissue from three donors. Hepatocytes were isolated by a collagenase perfusion method previously described (LeCluyse et al., 2005). Final cell viability prior to plating was determined by the Trypan Blue exclusion test and was greater than 75% in all cases.

Hepatocyte cultures were treated for three consecutive days with media containing dapagliflozin (0.2, 2 and 20 μ M), solvent (0.1% DMSO) controls or prototypical inducers. Rifampicin (RIF, 10 μ M), phenobarbital (PB, 1 mM) and 3-methylcholanthrene (3-MC, 2 μ M) were the prototypical inducers used as positive controls for the human hepatocyte

cultures. Both daily microscopic inspections of the cultures and monolayers and monitoring of lactate dehydrogenase leakage were employed as a measure of cytotoxicity. For RNA determination, cells under identical conditions were incubated for 48 hours. No cytotoxicity (changes in cell morphology or attachment) was observed during the incubation period. Following the three day treatment with test article and controls, cultures of hepatocytes from each treatment group were rinsed twice with ice-cold Hanks balanced salt solution (HBSS). Homogenization buffer (50 mM Tris-HCl, pH 7.0, 150 mM KCl, 2 mM EDTA) was added to each dish (0.5 mL/dish) and cells were scraped with a cell scraper. Harvested cells from each treatment were pooled and sonicated with a Vibra-Cell probe sonicator (Sonics & Materials, Danbury, CT) at 40 watts for 15-20 seconds. Cell lysates were centrifuged at 9,000g for 20 minutes at 4°C. Supernatants were collected and centrifuged at 100,000g for 60 minutes at 4°C. Final microsomal pellets were resuspended in 0.25 M sucrose with a Potter-Elvehjem style homogenizer fitted with a Teflon pestle. A small aliquot was taken for protein determination (BCA protein assay) and all samples were stored at -70°C. Microsomes were diluted in 100 mM potassium phosphate buffer at pH 7.4, spiked with marker substrate and were equilibrated to 37°C. Total incubation volumes were approximately 0.5 mL and all incubations were performed in triplicate. Metabolic reactions were initiated by the addition of NADPH (1 mM final concentration) and stopped at the indicated time points by addition of organic solvent. Samples were then extracted and analyzed for acetaminophen, hydroxybupropion, and 6 β -hydroxytestosterone. Following a 48 h incubation, cells from each treatment group were washed with HBSS, lysed with RLT buffer (Qiagen, Valencia, CA) and 1% β -mercaptoethanol, harvested, and

stored at -70°C until RNA analysis was done. RNA was isolated utilizing the RNeasy kits (Qiagen), and total RNA was quantified using a Nanodrop spectrophotometer.

Hepatocyte incubations. A stock solution of [^{14}C]dapagliflozin (5.6 mM) was prepared in ethanol. [^{14}C]Dapagliflozin, at a concentration of 30 μM , was incubated with fresh hepatocytes from mouse and cryopreserved hepatocytes from rat, dog, monkey and human for 3 h. A cell concentration of 1 million cells/mL was used. Control substrates 7-ethoxycoumarin and 7-hydroxycoumarin were incubated for 1 h at concentrations of 100 μM . Trypan blue exclusion was used to assess viability. The incubations were carried out in Krebs-Henseleit buffer (pH 7.4) for 3 h in a 37°C chamber which was maintained under an oxygen/carbon dioxide (95/5) and 95% humidity atmosphere. At the end of the incubation, two volumes of ACN were added to each sample. The samples were centrifuged at 2500xg for 10 min. A 100 μL portion of the supernatant was analyzed by LC/MS and scintillation counting. Extent of metabolism of dapagliflozin was calculated by comparing dapagliflozin concentration at 0 h versus 3 h. Cell viability and control substrate turnover were within acceptable limits.

Rat liver microsomal incubation to produce M12. A stock solution of dapagliflozin was prepared in ACN. Dapagliflozin, at a concentration of 0.98 mM, was incubated at 37°C for 5 h in a 250 mL mixture containing 0.1M potassium phosphate buffer (pH 7.4), 4.9 mM MgCl_2 , 6 mM NADPH, 0.48 mg/mL BSA, 580 unit/mL catalase, and 2 mg/mL protein of pooled rat liver microsomes. The incubation mixture was extracted three times with ethyl acetate (300 mL, 200 mL, then 200 mL). The combined ethyl acetate extract was

evaporated to dryness with a rotavapor, and the residue was dissolved in 3 mL of DMSO. After removal of insoluble material by centrifugation (12,000xg for 3 min), the DMSO solution was subjected to semipreparative HPLC separation.

Analysis. Samples from the Caco-2 permeability studies were analyzed on an HPLC system that consisted of the 2690 Waters separation module and a Waters 996 photodiode array detector (Waters, Milford, MA). The column used was YMC ODS-AQ 4.6 mm X 150 mm, 3 micron particle, maintained at 25°C and a flow rate of 1 mL/min. Caco-2 samples (100 µL) were injected without any sample preparation. An ACN:water gradient system was used for the separation. The amount of ACN in the gradient was increased in a stepwise fashion from 5% ACN to 90% ACN over 6 min, held for 7 min, then re-equilibrated to 5% ACN over 5 min. The mobile phases also contained 0.115% trifluoroacetic acid. Quantitation was based on the UV peak area of dapagliflozin (at 210 nm) in the samples.

Analysis of the metabolites from the probe substrates used in the microsomal incubations was conducted using assays that were developed and validated at Bristol-Myers Squibb Co. (Yao et al., 2007). Quantitation of the metabolites from the three probe substrates used in the CYP induction studies were conducted as described previously (LeCluyse et al., 2005). The analysis of metabolite profiles in hepatocytes was conducted on an HPLC system that consisted of two Shimadzu LC10AD pumps, a model SCL system controller, a model SIL 10 AD autoinjector, and a model SPD M10A diode-array detector (Shimadzu, Columbia, MD). The column used was Zorbax C18 (4.6 x 250 mm, 5 µm) column, run at ambient temperature and a flow rate of 0.8 mL/min. Hepatocyte samples were treated with two

volumes of ACN, vortexed, centrifuged at 2500xg for 10 min, and 25 μ L of supernatant was injected onto the LC/MS. The solvent systems used for the separation were composed of ACN and ammonium acetate (10 mM) in water, containing 0.1% formic acid. The amount of ACN in the gradient was increased in a stepwise fashion from 10% ACN to 45% ACN over 35 min, to 60% ACN over 5 min, held for 2 min, then re-equilibrated to 10% ACN over 10 min. The HPLC eluent was split, with 20% going to the mass spectrometer, and 80% collected for TopCount scintillation counting. The fraction collection interval on the TopCount was every 15s. Profiles were prepared by plotting net CPM values (CPM from column void volume were subtracted from CPM of subsequent fractions) against retention time. For analysis of positive controls in the hepatocyte study, the same HPLC system was used as above, but with a YMC ODS AQ C18 (2.0 x 50 mm, 3 μ m) column.

For the purification of M12 from a rat microsomal incubation, extract samples dissolved in DMSO were analyzed on an HPLC system equipped with a ASI-100 autosampler injector (Dionex Co., Sunnyvale, CA), a UVD 340 UV detector (Dionex Co.), two Varian Prep Star Mode 218 pumps (Varian Inc., Palo Alto, CA) and an ISCO Foxy 200 fraction collector (Teledyne Isco, Lincoln, NE). The column used was a YMC ODS-AQ, 20 x 150 mm, S5 (Waters, Milford, MA) and a flow rate of 10 mL/min was used. An ACN:water gradient system was used for the separation. The amount of ACN in the gradient was increased in a stepwise fashion starting with 10% ACN held for 5 min, then to 32% ACN over 2 min, held at 32% ACN for 13 min, then re-equilibrated to 10% ACN. M12 eluted around 17 min in this system. Fractions containing M12 were pooled and lyophilized.

For the analysis of dapagliflozin in preclinical samples, the HPLC system consisted of two Shimadzu LC10AD pumps (Shimadzu, Columbia, MD), a Perkin Elmer PE Series 200

autosampler (Perkin Elmer, CT), and a Hewlett Packard Series 1100 (Hewlett Packard Palo Alto, CA) heated column compartment. The column used was a ProntoSil C30 column, 2 mm x 50 mm, 5 μ m particles (Mac-Mod Analytical, Inc., Chadds Ford, PA), maintained at 60°C. Plasma and urine samples were treated with three volumes of ACN (containing a proprietary BMS compound as an internal standard), vortexed, centrifuged at 2500xg for 10 min, and 10 μ L of supernatant was injected onto the LC/MS. The solvent systems used for the separation were composed of ACN and ammonium acetate (10 mM) in water. The amount of ACN in the gradient was increased in a stepwise fashion from 0% ACN to 100% ACN over 6 min, held for 1.5 min, then re-equilibrated to 0% ACN over 1 min. The HPLC was interfaced to a Micromass triple quadrupole mass spectrometer (Micromass, Manchester, UK) equipped with an electrospray interface. Data acquisition employed multiple reaction monitoring (MRM). Positively charged ions representing the $[M+NH_4]^+$ for dapagliflozin and $[M+H]^+$ for the internal standard were selected in MS1 and collisionally dissociated with argon to form specific product ions which were subsequently monitored by MS2. The transitions monitored were m/z 426 \rightarrow 167 for dapagliflozin (ES^+) and m/z 459 \rightarrow 427 for IS.

The blood cell partitioning study with human blood was run at a later time, and the analysis of those samples utilized an HPLC system consisting of two Shimadzu LC10AD pumps (Shimadzu, Columbia, MD) and a Leap HTC PAL autosampler (LEAP technologies, Carrboro, NC). The column used was a YMS ODS (2 mm x 50 mm, 3 μ m particles, Waters Corp.), maintained at RT. Samples were treated with two volumes of ACN containing [$^{13}C_6$]dapagliflozin, vortexed, centrifuged at 2500xg for 20 min 4°C. Aliquots of 150 μ L in duplicate were transferred to a 96-well shallow filter plate (Millipore Corp.,

which was preloaded with 75 μ L of ACN, and stacked with a 96-deep well receiver plate. After centrifugation, 250 μ L of water was added to the receiver plate and mixed with the filtrate. The supernatant (10 μ L) was injected onto the LC/MS. The solvent systems used for the separation were composed of ACN and water. The amount of ACN in the gradient was increased in a stepwise fashion from 20% ACN to 80% ACN over 2.5 min, held for 0.3 min, then re-equilibrated to 20% ACN over 1.2 min. The HPLC was interfaced to a 4000 Q TRAP hybrid triple-quadrupole linear ion trap mass spectrometer equipped with a Turbo VTM source (Applied Biosystem, Foster City, CA), run in negative ionization mode. Data acquisition employed multiple reaction monitoring (MRM). Negatively charged ions representing the $[M-H]^-$ for dapagliflozin were selected in MS1 and collisionally dissociated with argon to form specific product ions which were subsequently monitored by MS2. The transitions monitored were m/z 407 \rightarrow 329 for dapagliflozin (ES^-) and m/z 413 \rightarrow 323 for [¹³C₆]dapagliflozin (IS).

For the analysis of dapagliflozin in the clinical samples, the HPLC system consisted of two Shimadzu LC10AD pumps (Shimadzu, Columbia, MD) and a Perkin Elmer PE Series 200 autosampler (Perkin Elmer, Waltham, MA). Samples were extracted from human plasma and urine using a Waters Oasis HLB solid-phase extraction well plate (Waters, Milford, MA). 150 μ L of plasma sample was pipetted into a 96-well plate, then 50 μ L of internal standard solution ([¹³C₆]dapagliflozin in ACN) and 200 μ L water was added. The Oasis SPE plate was conditioned according to manufacturer directions. Samples were loaded into the extraction wells, followed by 400 μ L of water, then 400 μ L of 10% methanol in water. Samples were eluted with 2 x 300 μ L of ACN. Eluate was evaporated at 40°C under nitrogen, and reconstituted in 100 μ L of 0.1% ammonium hydroxide in 10% ACN in

water. The sample was vortexed, centrifuged at 1500 x g for 3 min, and 10 μ L of supernatant was injected onto the HPLC. The chromatographic separation was carried out on a SunFire C18 column, 2.1 mm x 50 mm, 5 μ m particles (Waters, Milford, MA), and run at ambient temperature. The solvent systems used for the separation were composed of ACN and water. The amount of ACN in the gradient was increased in a stepwise fashion from 20% ACN to 30% over 0.5 min, then to 80% ACN over 2.5 min, held for 0.3 min, then re-equilibrated to 20% ACN over 0.2 min, and held for 1 min. The HPLC was interfaced to a Quattro Ultima mass spectrometer (Waters Corp, Manchester, UK) equipped with an electrospray interface, run in negative ionization mode. Data acquisition employed selective reaction monitoring (SRM). The transitions monitored were the same as those for the human blood cell partitioning study.

Plasma samples at 1, 4, and 12 h were profiled for metabolites using the same HPLC procedure as for the hepatocyte incubations (the total radioactivity measurements were BQL after 24 h, so the 48 and 144 h samples were not profiled). The plasma samples were loaded into the extraction wells, followed by 400 μ L of water, then 2 x 400 μ L of 10% methanol in water. Samples were eluted with 2 x 400 μ L of methanol. The eluted fractions were evaporated to dryness under nitrogen and reconstituted in 400 μ L of methanol/water (25:75, v/v). Following centrifugation, a 100 μ L portion was analyzed by HPLC for biotransformation profiling and mass spectral analysis. Radioactivity at the retention time correlating to the glucuronide conjugate of dapagliflozin M15 was also quantified and converted to concentration using a specific activity of 2.07 μ Ci/mg. Total radioactivity was determined in these plasma samples by liquid scintillation counting (LSC).

Pharmacokinetic data analysis. All plasma concentration vs. time data of dapagliflozin were analyzed by noncompartmental methods (Gibaldi, 1982) using the KINETICATM software program (Version 4.2, Thermo-Fisher Scientific, Waltham, MA). For the analysis of preclinical samples, the AUC_{0-n} and AUC_{tot} values were calculated using a combination of linear and log trapezoidal summations. The total body clearance (CL), mean residence time (MRT), half-life ($t_{1/2}$) and the steady state volume of distribution (V_{ss}) were calculated using noncompartmental methods after intravenous administration: $CL = \text{dose}/AUC_T$; $MRT = AUMC/AUC$; $t_{1/2} = MRT \cdot 0.693$; $V_{ss} = CL \cdot MRT$. Plasma clearance values were corrected for blood to plasma ratios, experimentally obtained in the various species, to compare blood clearance values to standard values for liver blood flow reported in the literature (Davies and Morris, 1993). V_{ss} values were compared to total body water reported for the various species (Davies and Morris, 1993). The absolute oral bioavailability (expressed as %) was estimated by comparing the ratio of dose-normalized AUC values after oral doses to those after intravenous doses. To obtain the percent of dose excreted in urine, the amount of dapagliflozin excreted in the urine in a given time interval was divided by the total dose given and multiplied by 100 to obtain the percentage of dose excreted in that interval. To calculate renal clearance (CL_R), the amount of drug excreted in the urine over a 24 h period was divided by AUC_{po}, and was compared to $GFR \cdot f_u$, to assess if net active renal transport was present (if $CL_R > GFR \cdot f_u$, net renal secretion is suggested; if $CL_R < GFR \cdot f_u$, net renal absorption is suggested). GFR values for the different species were obtained from the literature (Davies and Morris, 1993).

For the analysis of clinical samples, the slopes of the terminal phases of the plasma dapagliflozin, and plasma TRA concentration-time profiles, λ , was determined by log-

linear regression of at least three data points which yielded a minimum mean square error. The absolute values of λ were used to estimate the apparent terminal half-lives of plasma dapagliflozin and plasma TRA by: $t_{1/2} = 2/\lambda$. The areas under the plasma dapagliflozin and TRA concentration-time curves from zero extrapolated to infinite time, AUC_{tot}, were calculated by log- and linear-trapezoidal summations over the collection time, with the last quantifiable plasma concentration being divided by λ and the product added to the total area. The total apparent (oral) body clearance was calculated using $CL/F = \text{Dose}/\text{AUC}$. The calculated half-life is after an oral dose.

For the clinical urine samples, the percent of total radioactivity excreted in the urine was calculated as described above, based on the total radioactive dose. For dapagliflozin excretion, chromatographic separation of the dapagliflozin and scintillation counting was described in the above sections, and percentage of dose excreted was calculated as described above.

Prediction of CL and CL/F in humans. Allometric scaling was used to estimate the human clearance of dapagliflozin by using the body weight of the animal and the corresponding clearance values. The animal clearance values after correction for interspecies differences in plasma protein binding (not shown) were also used and that predicted clearance compared to the value from simple allometry. In order to compare the predicted clearance from allometry to the apparent clearance after an oral dose, the predicted clearance was divided by the average oral bioavailability of the animal species (64%).

Results

Caco-2 permeability and P-gp interactions. The permeability coefficient (P_c) of dapagliflozin in the apical to basolateral direction was 60 nm/sec at an initial concentration of 50 μ M at pH 7.4. This value is comparable to compounds that exhibit moderate absorption in humans (Marino et al., 2005). Under the same conditions, the average B-to-A P_c value of dapagliflozin was 227 nm/sec (BA/AB ratio of 3.8). In the presence of a P-gp inhibitor, the A-to-B permeability of dapagliflozin was 159 nm/sec and the B-to-A permeability was 188 nm/sec (BA/AB ratio decreased to 1.2). The BA/AB ratio of 3.8 and the decrease of P-gp mediated efflux (in the presence of a P-gp inhibitor) suggests that dapagliflozin may be a P-gp substrate.

To evaluate whether dapagliflozin inhibits the transport of P-gp substrates, the permeability of digoxin was measured across Caco-2 cell monolayers in the presence and absence of dapagliflozin at 10 μ M. Dapagliflozin showed weak inhibition of digoxin transport (10% at 10 μ M). The inhibition value for verapamil (a known P-gp inhibitor) was 65% at 10 μ M in this experiment. These results suggest the dapagliflozin is unlikely to be a P-gp inhibitor.

Plasma and serum protein binding. The plasma protein binding of dapagliflozin was determined by the equilibrium dialysis technique at 10 μ M and was found to be 95%, 93%, and 91% in rat, dog, and human, respectively. The serum protein binding of dapagliflozin in cynomolgus monkeys was determined by the ultrafiltration technique at 10 μ M and was found to be 91%. Control studies established that dapagliflozin was stable in rat, dog, monkey and human serum at 10 μ M for 4 hours at 37°C.

Blood cell partitioning. The blood to plasma ratios were found to be 0.71, 0.61, 0.73, and 0.88 in rat, dog, monkey, and human, respectively. These ratios reflect limited distribution of dapagliflozin to red blood cells.

Results from CYP inhibition in HLM. Dapagliflozin showed no relevant direct inhibitory effects on the activities of CYP1A2, CYP2A6, CYP2B6, CYP2C8, CYP2C9, CYP2C19, CYP2D6 and CYP3A4, as the IC₅₀ values were estimated to be greater than the highest concentration of dapagliflozin evaluated (45 μ M). The various known inhibitors that were incubated with the different CYP enzymes did show the expected inhibitory responses (data not shown).

CYP induction in human hepatocytes. There was no marked induction of CYP1A2, 2B6, or 3A4 when monitored by mRNA or enzyme activity, observed for dapagliflozin at the concentrations tested (0.2-20 μ M). The mRNA analysis as well as the enzyme activity revealed robust (10- to 26-fold) increases in hepatocyte cultures treated with positive controls (3-methylcholanthrene, phenobarbital, rifampicin) and little or no changes in cultures treated with dapagliflozin.

Metabolite profiles from hepatocyte incubations. Metabolite profiles of [¹⁴C]dapagliflozin after incubation for 3 h with hepatocyte preparations from mouse, rat, dog, monkey, and human are shown in Figure 1. Dapagliflozin was the major peak in all hepatocyte incubations. The extent of turnover of dapagliflozin in hepatocytes was 50% in rat, 26% in mouse, 24% in dog, 25% in monkey, and 10% in human. All metabolites observed in human hepatocyte incubations were also observed in the animal incubations. In human hepatocytes, M15 was the major metabolite, accounting for 2.1% of the total

radioactivity in the sample, with all other metabolites accounting for <0.9% of the total radioactivity.

Metabolites formed in incubations with hepatocytes were characterized by LC/MS/MS. The mass spectra of dapagliflozin and metabolites M8, M12, and M15 are shown in Figure 2. The evidence for the assignment of the structure of each metabolite is discussed below. Dapagliflozin gave an ammonia adduct ($M+NH_4^+$) and had an m/z of 426 Da. LC/MS/MS analysis showed product ions resulting from sequential losses of water: at m/z 391 from loss of 35 ($-H_2O, -NH_3$), at m/z 373 from loss of H_2O (18 Da) and at m/z 355 from loss of H_2O (18 Da). This retention time and mass spectra were identical to a matched authentic standard of dapagliflozin. Based on the m/z of 574 for the M2 ammonia adduct ($M+NH_4^+$), M2 was identified as a glucuronide conjugate arising after *O*-deethylation of dapagliflozin. LC/MS/MS could not reveal the site of conjugation as being the phenol moiety. LC/MS/MS data could not be obtained for metabolite M4, due in part to its low abundance in rodent hepatocytes. Metabolite M8 was identified as the *O*-deethylated phenol arising from dealkylation of dapagliflozin since it exhibited the same retention time, m/z of 398 for the ammonia adduct, and mass spectra as those of the authentic phenol standard (BMS-511926). M10 was tentatively identified as a glucuronide conjugate of dapagliflozin since the ammonia adduct of M10 had an m/z of 602 and LC/MS/MS analysis revealed a product ion at m/z of 391 arising from loss of 176 Da (suggestive of a glucuronide moiety) and 35 Da ($-NH_3, -H_2O$). M12 was tentatively identified as a hydroxylation product of dapagliflozin since the ammonia adduct of M12 had an m/z of 442 and LC/MS/MS analysis showed product ions at m/z 407 from loss of 35 Da. Purification of the material from a large scale incubation of dapagliflozin with rat liver microsomes allowed

identification of the metabolite as a product of benzylic hydroxylation (BMS-639432), although the stereochemistry at the site of modification was not assigned. M15 was also identified as a glucuronide conjugate of dapagliflozin since the ammonia adduct of M15 had an m/z of 602 and a LC/MS/MS analysis showed product ions at m/z 409 from a loss of 193 Da, which was due to loss of NH_3 (17 Da) and glucuronide (176 Da). The ammonia adduct of M15a had an m/z of 442 (16 mass units greater than the ammonia adduct of dapagliflozin), which appeared to be an oxidative metabolite, but were not otherwise characterized. The ammonia adduct of M16 had an m/z of 440 (14 mass units greater than the ammonia adduct of dapagliflozin). From its mass spectra, the cleavage of the sugar ring to form an m/z of 289 confirms that the oxidation could only occur on the hydroxymethyl group of the sugar ring. Thus M16 was tentatively identified as an oxidative metabolite of dapagliflozin. This peak was not adequately separated from dapagliflozin to allow quantification, however it was judged to be very minor in separate analysis of select samples with radioflow detection.

Pharmacokinetics and bioavailability of dapagliflozin after single doses in rats, dogs, and monkeys. The main pharmacokinetic parameters for dapagliflozin for all species tested are summarized in Table 1 and the plasma profiles are shown in Figure 4. The clearance values reported in Table 1 are plasma clearance values, which below are corrected for blood to plasma ratios, for comparison to liver blood flows.

In the rat, the systemic blood clearance of dapagliflozin was 6.8 ± 0.8 mL/min/kg, which is ~ 12 % of hepatic blood flow. The blood clearance was calculated by dividing the plasma clearance by the blood to plasma ratio; for rat those values were 4.8 mL/min/kg, and a ratio of 0.71. The steady state volume of distribution was high (1.6 ± 0.1 L/kg), compared to

0.7 L/kg for total body water in the rat, indicating extravascular distribution. The estimated elimination half-life after IA administration was 4.6 ± 0.8 h and the mean residence time was 5.6 ± 0.9 h. The oral bioavailability of dapagliflozin was 84%. The time to reach peak concentrations (T_{max}) after an oral dose was 1.7 ± 2.0 h.

In the dog, the systemic blood clearance of dapagliflozin was 2.5 ± 0.3 mL/min/kg, which is ~ 8 % of hepatic blood flow in the dog. The steady state volume of distribution was 0.8 ± 0.1 L/kg, similar to total body water in the dog (0.6 L/kg), indicating modest extravascular distribution. The estimated elimination half-life after IV administration was 7.4 ± 1.2 h and the mean residence time was 9.3 ± 0.7 h. The oral bioavailability of dapagliflozin was $83 \pm 2\%$. The T_{max} after an oral dose was 0.6 ± 0.4 h. The percent of dose excreted in the urine as dapagliflozin, over a 24 hour period, was 3.4 ± 0.2 % after an oral dose of 6.6 mg/kg. The CL_R was 0.7 mL/min, and $GFR \cdot f_u$ was 4.3 mL/min.

In the monkey, dapagliflozin was cleared more quickly than in the dog, with a systemic blood clearance of 8.8 ± 3.1 mL/min/kg, about 20 % of hepatic blood flow in the monkey. The steady state volume of distribution was 0.8 ± 0.2 L/kg, similar to total body water (0.7 L/kg), indicating modest extravascular distribution. The estimated elimination half-life was after IV administration was 3.5 ± 1.9 h and the mean residence time was 2.2 ± 0.5 h. The oral bioavailability of dapagliflozin was 25 ± 2 %. The T_{max} after an oral dose was 1.9 ± 1.8 h. The percent of dose excreted in the urine as dapagliflozin, over a 24 hour period was $3.8 \pm 0.3\%$ after an oral dose of 6 mg/kg. The CL_R was 5.7 mL/min, and $GFR \cdot f_u$ was 0.9 mL/min.

Prediction of pharmacokinetics in humans. The human systemic plasma clearance was predicted to be 2.1 mL/min/kg from simple allometry ($CL = 4.26 \cdot BW^{0.83}$, $R^2 = 0.87$, Figure 5). Utilizing the blood to plasma ratio of 0.88 in human serum, this is a blood clearance of 2.4 mL/min/kg, corresponding to 11% of hepatic blood flow. The plasma clearance, when divided by the average bioavailability across the animal species (64%), corresponds to a predicted oral clearance of 3.3 mL/min/kg. The systemic plasma clearance value after correction for protein binding was 1.9 mL/min/kg (oral clearance of 3.0 mL/min/kg). Correction of the plasma clearance with metabolism rates was not done, given the interspecies differences in metabolite profiles in hepatocytes.

Pharmacokinetics of dapagliflozin after a single dose to humans. Dapagliflozin was rapidly absorbed after oral administration of the 50 mg dose with maximum plasma concentrations (C_{max}) attained within 1 hour after administration in a fasted state (Table 1). The mean terminal half-life ($T_{1/2}$) value for dapagliflozin was 13.8 h. The observed oral plasma clearance was 4.9 mL/min/kg. The amount of total radioactivity recovered in the urine was 75.2%; the amount of unchanged dapagliflozin recovered in urine was 1.6%. The CL_R was 5.6 mL/min and $GFR \cdot f_u$ was 10.8 mL/min.

Figure 6 shows the plasma profile of dapagliflozin compared to plasma profile of total radioactivity. The levels of total radioactivity were approximately 3- fold higher than the levels of dapagliflozin. Five timepoints, at 1, 4, 12, 48, and 144 h were sampled for biotransformation analysis. Dapagliflozin and M15 levels were quantitated as described in the methods section. Timepoints after 96 h were below the lower limit of quantitation (BQL) for dapagliflozin. The total radioactivity measurements were BQL after 24 hr. Figure 7 shows the levels of dapagliflozin and M15 compared to the total radioactivity, at

DMD 29165

1, 4, and 12 h. The sum of dapagliflozin + M15 concentrations accounted for >72 % of the total plasma radioactivity at all time points.

Discussion

Optimal treatment for hyperglycemia in type 2 diabetes still remains a major clinical challenge. Inhibition of SGLT offers great potential as a novel mode of treating hyperglycemia, without some of the common side effects and stress on beta cells, thus progression of the disease may possibly be altered with this class of drugs. Because of the side effects of nonselective inhibition of SGLT and enzymatic instability of *O*-glucoside inhibitors in many tissues, there is a medical need for more hydrolytically stable C-glucosides which are SGLT2-selective, such as dapagliflozin.

In order to aid in compound selection and to determine whether dapagliflozin was a suitable compound for progression into the clinic, the pharmacokinetics in animals and important ADME parameters were obtained. The plasma clearance of dapagliflozin was low in the three species investigated. The volume of distribution values ranged from total body water in the dog and monkey to about 2-fold total body water in the rat. The elimination half lives were moderate in the rat (4.6 h) and dog (7.4 h) but lower in the monkey (3.5 h). The plasma and serum (monkey) protein binding for dapagliflozin was found to be moderate to high, ranging from 91% to 95% in preclinical species, and 91% in humans. Bioavailability values ranged from >80% in the rat and dog to 25% in the monkey. The predicted oral clearance using the clearance values from simple allometry was 3.3 mL/min/kg, based on an average bioavailability value calculated from the different species.

The intrinsic permeability seen for dapagliflozin across Caco-2 cells was comparable to compounds that exhibit good absorption in humans (Marino et al., 2005), and would

indicate good systemic bioavailability of the compound after oral administration. The efflux ratio of 3.8 seen in Caco-2 cells suggests that dapagliflozin may be a P-gp substrate, but it exhibits high intrinsic permeability in the Caco-2 cells and good bioavailability in rats and dogs, and thus absorption and bioavailability were predicted to be adequate in humans. It is possible that the doses in rats and dogs were enough to saturate the P-gp transporter at the level of the intestinal lumen and lead to the observed good bioavailability, however, dapagliflozin demonstrated linear pharmacokinetics over a very large dose range in both species so it is more likely that passive permeability dominates the absorption of the compound. P-gp can play a role in drug disposition at the level of the kidney (Li et al., 2006). While the comparison of $GFR \cdot fu$ to CL_R for monkeys and dogs does indicate that some active renal processes may be occurring, it should be noted that the urinary excretion of dapagliflozin is very low in all species, so the action of P-gp on the disposition of dapagliflozin at the renal level may not be relevant. And while the bioavailability in the monkey is much lower than in other species, factors other than renal transport are governing the lower oral exposure.

In incubations with human hepatocytes, a glucuronide conjugate (M15) of dapagliflozin was found to be the major metabolite. Glucuronides of dapagliflozin (M15 and M10) were also found in the animal hepatocyte incubations. Dapagliflozin was not found to be an inhibitor or an inducer of CYP enzymes. The overall favorable ADME properties of dapagliflozin in animals, the favorable predicted parameters in humans, and the overall safety and efficacy of the compound in preclinical testing led to the progression of the compound into clinical trials (List et al., 2008; Komoroski et al., 2009 (a); Komoroski et al., 2009 (b)).

Dapagliflozin, administered to healthy subjects as an oral solution of 50 mg, was rapidly absorbed from the gastrointestinal tract with $T_{max} < 1$ h, and appeared to be safe and well-tolerated. Based on the urinary recovery of total radioactivity in that study, the systemic absorption of orally administered dapagliflozin was at least 75% within 24 h of dosing (data not shown). Thus P-gp does not appear to be limiting the absorption of dapagliflozin in humans. The urinary excretion of (parent) dapagliflozin is very low, thus the contribution of renal clearance to the total clearance of dapagliflozin is very small.

In plasma, the ratio of the dapagliflozin concentration to the TRA at any one time point was approximately 0.3 of TRA, suggesting that metabolites account for a significant portion of dapagliflozin-related compounds in the plasma. Indeed, the major metabolite identified in human hepatocytes was also found to be a major circulating metabolite in the clinical samples. This non-pharmacologically active glucuronide conjugate, M15 (further characterization to be discussed in a future publication), was found in human plasma at concentrations similar to dapagliflozin. M15 was cleared similarly to dapagliflozin as indicated by the comparable slopes of their elimination phases. Levels of M15 were significant in all species used for toxicological evaluation (data not shown) relative to levels in humans.

Allometry rather than in vitro data was used to predict human clearance for a number of reasons. Clearance predictions from microsomal incubations with NADPH, accounting for only oxidative metabolism, or from microsomal incubations with UDPGA were not done as the predicted clearance values often underpredict observed values for drugs cleared by glucuronidation and are highly dependent on incubation conditions (Kilford, et al., 2009). Although hepatocytes have been shown to produce better predictive results for drugs

cleared by glucuronidation, the preclinical studies with hepatocytes did not give enough dapagliflozin turnover to reliably determine an intrinsic clearance. Thus, allometry was used as a reasonable alternative. The oral clearance (3.3 mL/min/kg) predicted from simple allometry is quite close to the observed value (4.9 mL/min/kg); correcting for protein binding resulted in a very similar prediction of oral clearance (3.0 mL/min/kg). Dapagliflozin is a low clearance compound in humans.

In summary, dapagliflozin is a potent inhibitor of SGLT2, and shows a reduction in plasma glucose in animal models (Han et al., 2008; Meng et al., 2008). The preclinical characteristics and pharmacokinetics of dapagliflozin supported its progression into clinical trials, with no unusual drug-drug interaction potential or distribution properties being demonstrated. This novel compound looks very promising as an additional therapy for hyperglycemia, with the potential of becoming a major therapy.

Acknowledgments: We acknowledge the contributions of Jinnan Cai from BMS Bioanalytical Sciences, Princeton, NJ, for excellent analytical support; Dr. Sam Bonacorsi and Mr. Kai Cao from BMS Radiochemistry, New Brunswick, NJ, for providing the labeled dapagliflozin for studies, and Dr. Aberra Fura, Dr. Praveen Balimane, and Dr. Punit Marathe for their helpful comments on this manuscript.

References

- Barnett A (2006) DPP-4 inhibitors and their potential role in the management of type 2 diabetes *Int J Clin Pract* **60**:1454-1470.
- Davies B and Morris T (1993) Physiological parameters in laboratory animals and humans *Pharm Res* **10**(7):1093-1095.
- Deetjen P, von Baeyer H and Drexel H (1992) Renal glucose transport. In *The Kidney: Physiology and Pathophysiology* (Seldin DW and Giebisch G eds) pp 2873-2888, Raven Press, Ltd., New York.
- Edelman SV (1998) Importance of glucose control. *Med Clin North Am* **82**:665-687.
- Ellsworth BA, Meng W, Patel M, Girotra RN, Wu G, Sher PM, Hagan DL, Obermeier MT, Humphreys WG, Robertson JG, Wang A, Han S, Waldron TL, Morgan NN, Whaley JM, and Washburn WN (2008) Aglycone exploration of C-arylglucoside inhibitors of renal sodium-dependent glucose transporter SGLT2 *Bioorg Med Chem Lett* **18**:4770-4773.
- Ehrenkranz JRL, Lewis NG, Kahn CR and Roth J (2005) Phlorizin: a review. *Diabetes Metab Res Rev* **21**:31-38.
- Gibaldi M (1982) Noncompartmental analysis based on statistical moment theory in *Pharmacokinetics* (Gibaldi M and Perrier D eds) pp 409-417, Marcel-Dekker, Inc.; New York.
- Han S, Hagan DL, Taylor JR, Xin L, Meng W, Biller SA, Wetterau JR, Washburn WN, Whaley JM (2008) Dapagliflozin, a selective SGLT2 inhibitor, improves glucose homeostasis in normal and diabetic rats *Diabetes* **57**:1723-1729.
- Jonas J-C, Sharma A, Hasenkamp W, Ilkova H, Patanè G, Laybutt R, Bonner-Weir S, and Weir GC (1999). Chronic hyperglycemia triggers the loss of pancreatic β cell differentiation in an animal model of diabetes. *J Biol Chem* **274**:14112-14121.
- Kamath A, Wang J, Lee FY, and Marathe P (2008) Preclinical pharmacokinetics and in vitro metabolism of dasatinib (BMS-354825): a potent oral multi-targeted kinase inhibitor against SRC and BCR-ABL. *Cancer Chemother Pharmacol* **61**:365-376.
- Kanai Y, Lee WS, You G, Brown D and Hediger MA (1994) The human kidney low affinity Na(+)/glucose cotransporter SGLT2. Delineation of the major renal reabsorptive mechanism for D-glucose. *J Clin Invest* **93**:397-404.
- Kilford PJ, Stringer R, Sohal B, Houston BJ, and Galetin A (2009) Prediction of drug clearance by glucuronidation from in vitro data: use of combined cytochrome P450 and UDP-glucuronosyltransferase cofactors in alamethicin-activated human liver microsomes. *Drug Metab. Disp.* **37**: 82-89
- Komoroski B, Vachharajani N, Feng Y, Li L, Kornhauser D, and Pfister M (2009) Dapagliflozin, a novel, selective SGLT2 inhibitor, improved glycemic control over 2 weeks in patients with type 2 diabetes mellitus. *Clin Pharmacol Ther* **85**:513-519.

Komoroski B, Vachharajani N, Boulton D, Kornhauser D, Geraldles M, Li L, and Pfister M (2009) Dapagliflozin, a novel SGLT2 inhibitor, induces dose-dependent glucosuria in healthy subjects. *Clin Pharmacol Ther* **85**:520-526.

LeCluyse E, Alexandre E, Hamilton GA, Viollon-Abadie C, Coon DJ, Jolley S, and Richert L (2005) Isolation and culture of primary human hepatocytes. *Methods Mol Biol* **290**:207-229.

Li M, Anderson GD, and Wang J (2006) Drug-drug interactions involving membrane transporters in the human kidney. *Expert Opinion Drug Metab Toxicol* **2**:505-532.

List JF, Woo VC, Morales E, Tang W, and Fiedorek FT (2009) Sodium-glucose co-transport inhibition with dapagliflozin in type 2 diabetes mellitus. *Diabetes Care* **32**:650-657.

Marino AM, Yarde M, Patel H, Chong S, and Balimane P (2005) Validation of the 96 well Caco-2 cell culture model for high throughput permeability assessment of discovery compounds. *Intl J Pharmaceut* **297**:235-241.

Meng W, Ellsworth BA, Nirschl AA, McCann PJ, Patel M, Girotra RN, Wu G, Sher PM, Morrison EP, Biller SA, Zahler R, Deshpande PP, Pullockaran A, Hagan DL, Morgan N, Taylor JR, Obermeier MT, Humphreys WG, Khanna A, Discenza L, Robertson JR, Wang A, Han S, Wetterau JR, Janovitz EB, Flint OP, Whaley JM, and Washburn WN (2008) Discovery of Dapagliflozin: a potent, selective renal sodium-dependent glucose cotransporter 2 (SGLT2) inhibitor for the treatment of Type 2 Diabetes. *J Med Chem* **51**: 1145-1149.

Mohler ML, He Y, Wu Z, Hwang DJ, and Miller DD (2008) Recent and Emerging Anti-Diabetes Targets. *Medicinal Res Rev* **29**: 125-195.

Nesto RW, Bell D, Bonow RO, Fonseca V, Grundy SM, Horton ES, Le Winter M, Porte D, Semenkovich CF, Smith S, Young LH, and Kahn, R (2004) Thiazolidinedione use, fluid retention, and congestive heart failure: a consensus statement from the American Heart Association and American Diabetes Association. *Diabetes Care* **27**:256-263.

Oku A, Ueta K, Arakawa K, Ishihara T, Nawano M, Kuronuma Y, Matsumoto M, Saito A, Tsujihara K, Anai M, Asano T, Kanai Y and Endou H (1999) T-1095, an inhibitor of renal Na⁺-glucose cotransporters may provide a novel approach to treating diabetes. *Diabetes* **48**:1794-1800.

Porte D (2001) Clinical importance of insulin secretion and its interaction with insulin resistance in the treatment of type 2 diabetes mellitus and its complications. *Diabetes Metab Res Rev* **17**:181-188.

Rotella DP (2004) Novel “second generation” approaches for the control of Type 2 diabetes. *J Med Chem* **47**:4111-4112.

Seglen PO (1976) Preparation of isolated rat liver cells. *Methods Cell Biol* **13**: 29-83.

Skyler JS (2004) Diabetes Mellitus: Pathogenesis and Treatment Strategies. *J Med Chem* **47**:4113-4117.

Turk E, Zabel B, Mundlose S, Dyer J, Wright EM (1991) Glucose/galactose malabsorption caused by a defect in the Na⁺/glucose cotransporter *Nature* **350**:354-356.

Wallner EI, Wada J, Tramonti G, Lin S and Kanwar YS (2001) Status of glucose transporters in the mammalian kidney and renal development *Ren Fail* **23**:301-310.

Wright EM, Hirayama B, Hazama A, Loo DD, Supplisson S, Turk E and Hages KM (1993) The sodium/glucose cotransporter (SGLT1). *Soc Gen Physiol Ser* **48**:229-241.

Yao M, Zhu M, Sinz M, Shang H, Humphreys WG, Rodrigues D and Dai R (2007). Development and full validation of six inhibitor assays for five major cytochrome P450 enzymes in human liver microsomes using an automated 96-well microplate incubation format and LC-MS/MS analysis. *J Pharmaceutical Biomedical Analysis* **44**:211-223.

Legends for Figures

- Fig. 1. Metabolite profiles of [^{14}C]dapagliflozin after incubation with hepatocytes from A) human, B) mouse, C) rat, D) dog, and E) monkey
- Fig. 2. Positive-ion MS/MS spectra of A) dapagliflozin and 3 major metabolites, B) M8 (BMS-511926), C) M12 (BMS-639432), and D) M15 (dapagliflozin glucuronide), observed in hepatocytes. Refer to Figure 3 for the assignment of fragments.
- Fig. 3. Metabolic pathway for dapagliflozin in hepatocytes; fragment assignments for dapagliflozin and metabolites.
- Fig. 4. Dapagliflozin concentrations in plasma of A) rats, B) dogs, and C) monkeys after IV or IA and PO administration of 1 mg/kg, 6.6 mg/kg, and 6 mg/kg, respectively. Each point represents the mean of three determinations.
- Fig. 5. Allometric scaling plot of plasma clearance values from preclinical species.
- Fig. 6. Dapagliflozin and total radioactivity in human plasma after oral administration of a single 50 mg dose of [^{14}C]dapagliflozin. Each point represents the mean of six subjects.
- Fig. 7. Dapagliflozin, M15, and total radioactivity in human plasma at selected timepoints where M15 was analyzed, after oral administration of a single 50 mg dose of [^{14}C]dapagliflozin.

TABLE 1

Pharmacokinetic parameters of dapagliflozin in preclinical species after single intravenous or oral doses and in humans after single oral dose

Species	Route	Dose ^a (mg/kg)	Cmax (µg/mL)	Tmax (h)	AUC _{tot} (µg•h/mL)	t _{1/2} (h)	CL _p (mL/ min/kg)	V _{ss} (L/kg)	F (%)
Rat	IA	1	-	-	3.55±0.42	4.6±0.8	4.8±0.6	1.6±0.1	84±21
	PO	1	0.60±0.46	1.7±2.0	2.96±0.73	-	-	-	
Dog	IV	6.6	-	-	76.4±10.1	7.4±1.2	1.5±0.2	0.8±0.1	83±2
	PO	6.6	10.7±1.6	0.6±0.4	63.6±7.3	-	-	-	
Monkey	IV	6	-	-	17.1±6.8	3.5±1.9	6.4±2.3	0.8±0.2	25±2
	PO	6	1.54±0.40	1.9±1.8	4.27±2.17	-	-	-	
Human ^b	PO	50 mg	0.55±0.02	0.5 (0.5-0.75)	2.43±0.03	13.8±9.4	4.9±0.2 ^c	- ^d	- ^d

^a Dosing vehicle used in preclinical pharmacokinetic studies was polyethylene glycol-400/water/ethanol (45/45/10); in clinical study the dose was administered as a pressed tablet.

^b Urinary excretion of dapagliflozin (after an oral dose) in dogs was 3.4 ± 0.2%; in monkeys was 3.8 ± 0.3%, and in humans was 1.6 ± 0.8 % of the total dose. Urinary excretion was not measured in rats.

^c CL/F (observed).

^d V_{ss}, F were not calculated in humans, as there was not IV data.

Fig 1

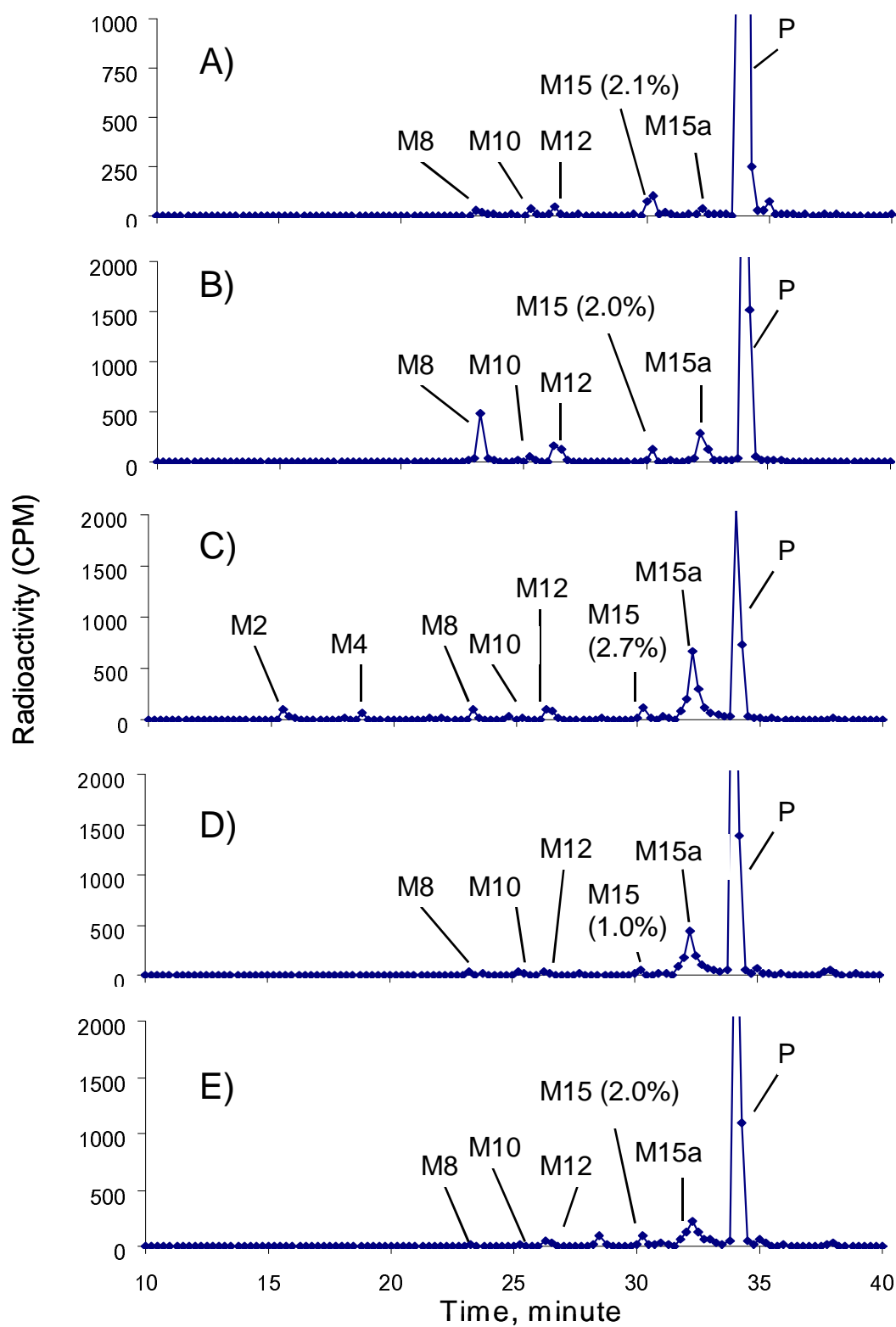


Fig 2

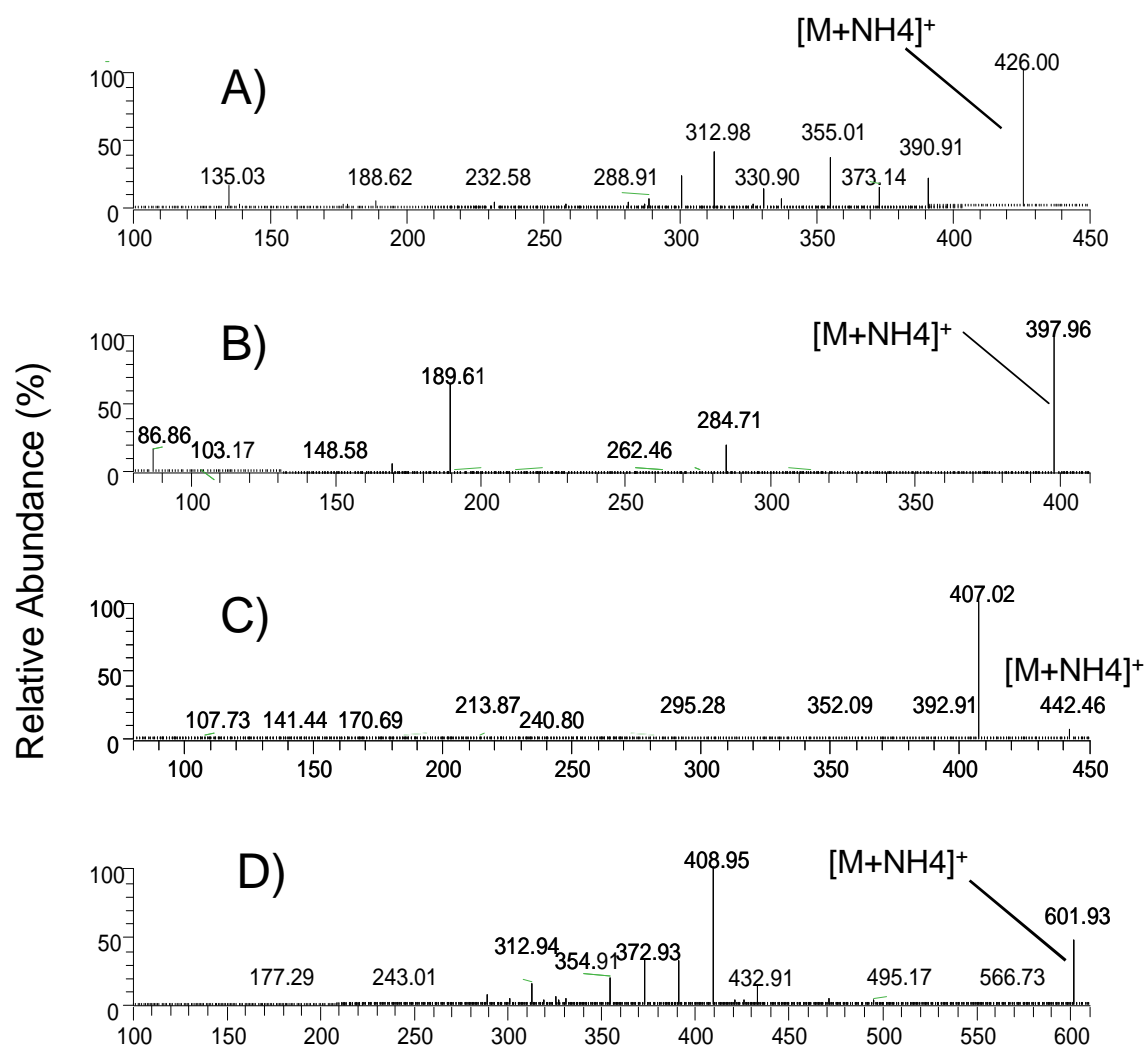


Fig 3

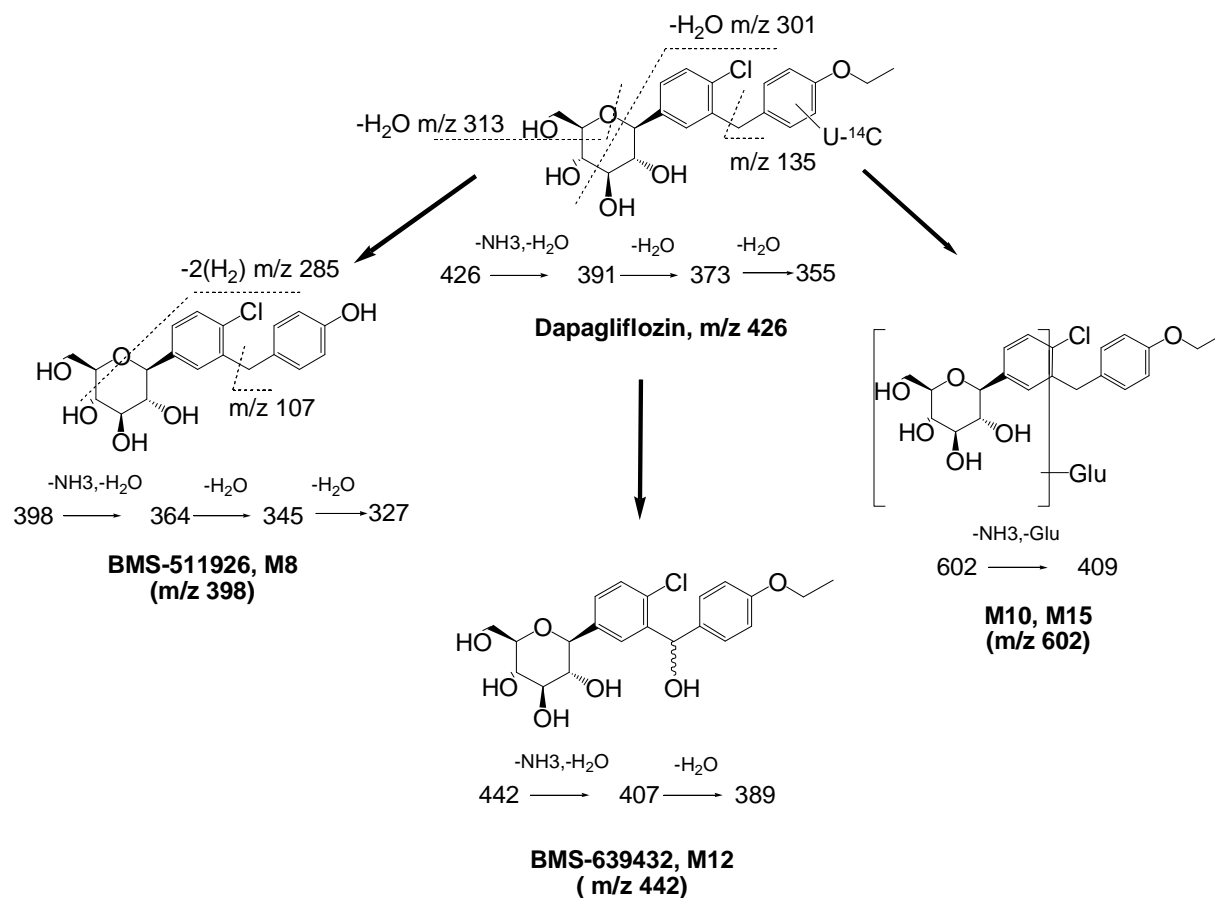


Fig 4

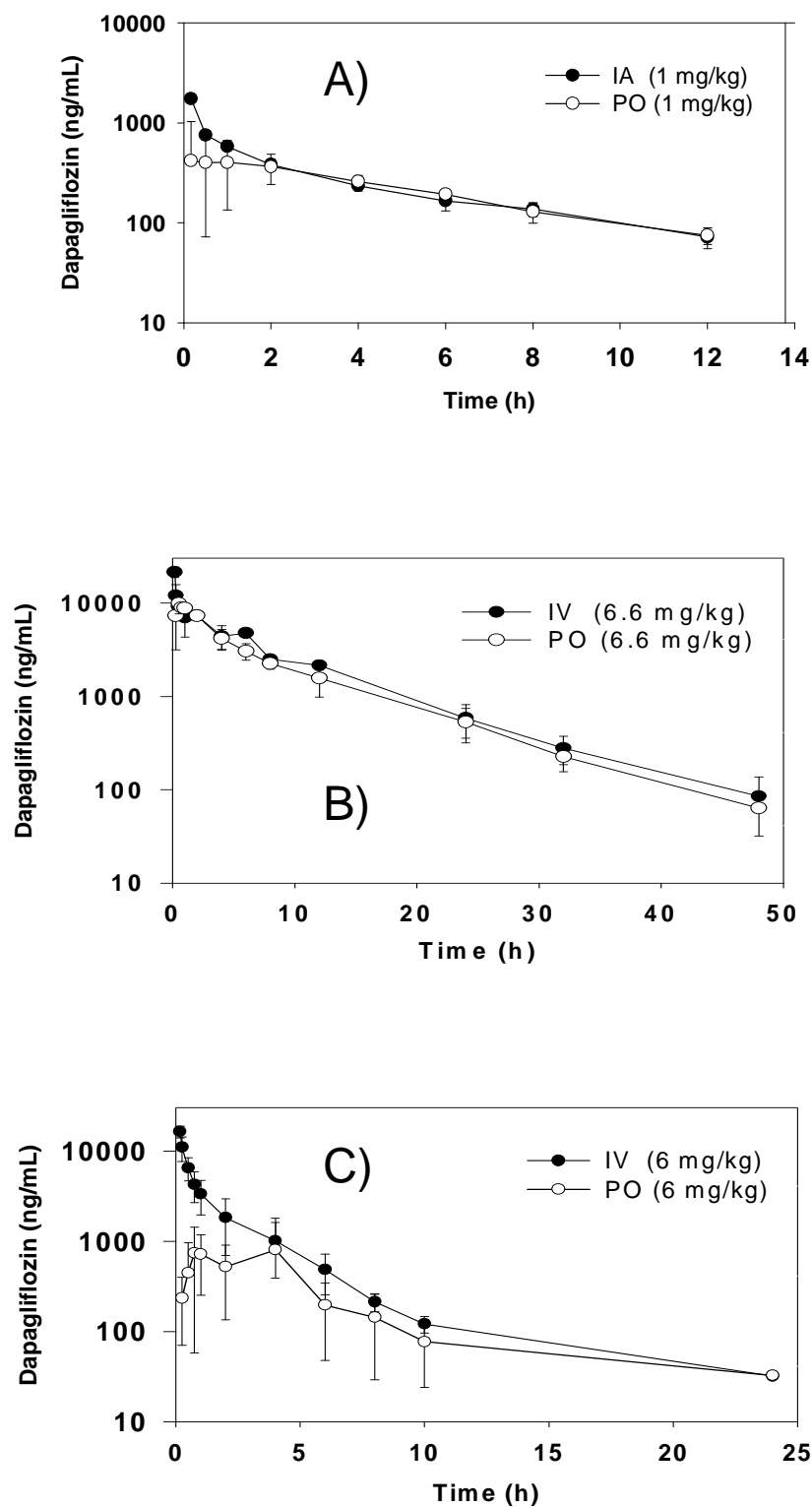


Fig 5

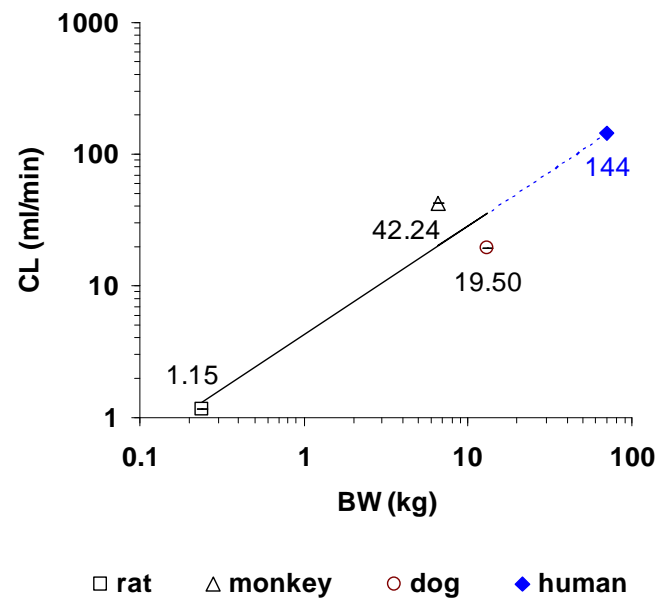


Fig 6

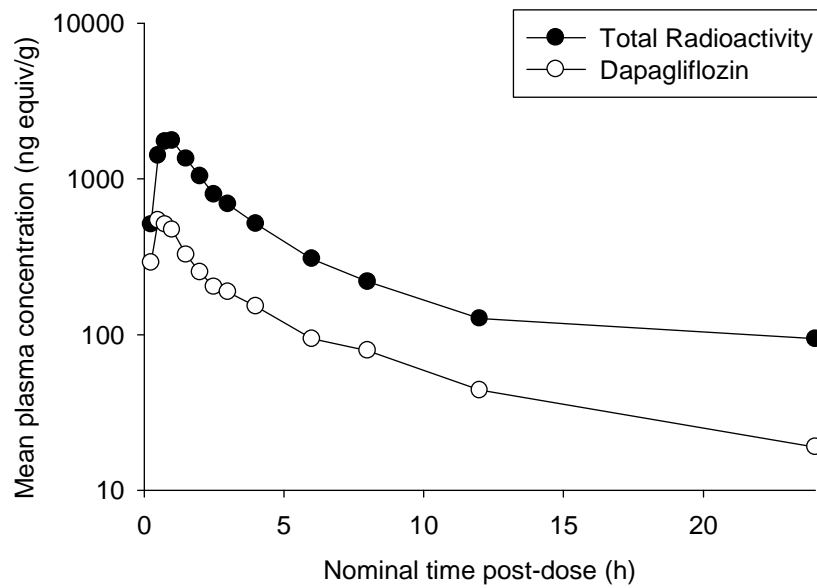


Fig 7

